J Comput Aided Mol Des (2008) 22:19–28
DOI 10.1007/s10822-007-9149-4

An eleven amino acid residue deletion expands the substrate specificity of acetyl xylan esterase II (AXE II) from *Penicillium purpurogenum*

Marcela Colombres · José A. Garate · Carlos F. Lagos · Raúl Araya-Secchi · Patricia Norambuena · Soledad Quiroz · Luis Larrondo · Tomas Pérez-Acle · Jaime Eyzaguirre

Received: 5 July 2007 / Accepted: 12 November 2007 / Published online: 1 December 2007

Abstract The soft-rot fungus *Penicillium purpurogenum* secretes to the culture medium a variety of enzymes related to xylan biodegradation, among them three acetyl xylan esterases (AXE I, II and III). AXE II has 207 amino acids; it belongs to family 5 of the carbohydrate esterases and its structure has been determined by X-ray crystallography at 0.9 Å resolution (PDB 1G66). The enzyme possesses the α/β hydrolase fold and the catalytic triad typical of serine esterases (Ser90, His187 and Asp175). AXE II can hydrolyze esters of a large variety of alcohols, but it is restricted to short chain fatty acids. An analysis of its three-dimensional structure shows that a loop that covers the active site may be responsible for this strict specificity. Cutinase, an enzyme that hydrolyzes esters of long chain fatty acids and shows a structure similar to AXE II, lacks this loop. In order to generate an AXE II with this broader specificity, the preparation of a mutant lacking residues involving this loop (Gly104 to Ala114) was proposed. A set of molecular simulation experiments based on a comparative model of the mutant enzyme predicted a stable structure. Using site-directed mutagenesis, the loop's residues have been eliminated from the AXE II cDNA. The mutant protein has been expressed in *Aspergillus nidulans* A722 and *Pichia pastoris*, and it is active towards a range of fatty acid esters of up to at least 14 carbons. The availability of an esterase with broader specificity may have biotechnological applications for the synthesis of sugar esters.

Keywords Acetyl xylan esterase · Cutinase · Comparative modeling · Mutagenesis · *Penicillium purpurogenum*

Introduction

Hemicelluloses are a set of amorphous polysaccharides present in plant cell walls in association with cellulose and lignin, and constitute about 30% of lignocellulose [1]. The main component of the hemicelluloses is xylan. This glycan is composed of a linear chain of xylose residues linked β (1→4) and presents a variety of substituents in carbons 2 and 3 of the xyloses, their type and amount depending on its source. Joined by glycosidic linkages are L-arabinoses and methyl glucuronate, while acetate is bound by ester linkages. In addition, hydroxycinnamic acids (mainly ferulic and *p*-coumaric acids) are found in ester linkages to the arabinose substituents [2].

The biodegradation of xylan is performed by a number of bacteria and fungi. It is a complex process requiring the concerted action of several glycanases and esterases, mainly extracellular, which attack the main chain and the substituent linkages [3]. Among them are the acetyl xylan

Marcela Colombres and José A. Garate have equally contributed to this work.

Electronic supplementary material The online version of this article (doi:10.1007/s10822-007-9149-4) contains supplementary material, which is available to authorized users.

M. Colombres · P. Norambuena · S. Quiroz · L. Larrondo · J. Eyzaguirre
Departamento de Genética Molecular y Microbiología, Pontificia Universidad Católica de Chile, Casilla 114-D, Santiago, Chile

J. A. Garate · C. F. Lagos · R. Araya-Secchi · T. Pérez-Acle
Centre for Bioinformatics (CBUC), Pontificia Universidad Católica de Chile, Casilla 114-D, Santiago, Chile

J. Eyzaguirre (✉)
Universidad Andrés Bello, República, 217 Santiago, Chile
e-mail: jeyzaguirre@unab.cl

esterases (AXE; E.C. 3.1.1.72), which hydrolyze the acetate residues, and constitute the purpose of this work.

AXEs have been identified, purified and characterized from several microorganisms [4]. Among them is *Penicillium purpurogenum*, a soft-rot actinomycete which produces a large number of xylanolytic enzymes [5] including three AXEs, identified as AXE I, II and III. AXE I has been characterized and sequenced and belongs to family 1 of the carbohydrate esterases [6]. AXE III is currently under study, while AXE II has been sequenced [7] and its three-dimensional structure determined by X-ray crystallography [8, 9]. The three enzymes have basically similar substrate specificity: they hydrolyze esters of short chain fatty acids but they tolerate a wide variety of alcohol moieties [10].

AXE II is a monomeric non-glycosylated protein. The mature protein consists of 207 amino acid residues and has a calculated molecular mass of 20,665 in good agreement with the value of 23,000 estimated by SDS-PAGE. Its pI is 7.8 and shows a pH optimum of 6.0 and a temperature optimum of 60 °C [7, 10]. The enzyme belongs to family 5 of the carbohydrate esterases. Its three-dimensional structure (determined to a resolution of 0.9 Å) consists of a doubly wound α/β sandwich with a central parallel β-sheet of six strands with two α-helices on each side. It possesses 10 Cys residues forming five disulfide bridges and the catalytic triad, typical of serine esterases is conformed by Ser90, His187 and Asp175. It has only a catalytic domain and does not bind cellulose or xylan [8, 9].

The tertiary structure of AXE II is similar to that of the cutinase from the phytopathogenic fungus *Fusarium solani* (Fig. 1a–c). This last enzyme, also a serine esterase, has an amino acid chain of 197 residues and four cysteines forming two S–S bridges which are essential for activity [11]. Cutinases are hydrolases which degrade cutin, a polyester which is deposited in the outer surface of the leaves and stems of plants. Cutin is composed of interesterified hydroxy and epoxy-hydroxy C16 and C18 fatty acids. Cutinase differs, therefore, from AXE II in that it can hydrolyze long chain fatty acid esters. If the structure of both enzymes is compared at the active site, the position of the catalytic triad is similar. However, AXE II possesses a loop ($\lambda 3$) located in the rear wall of the active site which is absent in cutinase. If the sequences of both enzymes are aligned (Fig. 2), two major gaps are found in the cutinase sequence. One of these, a 14 residues gap, fits in line with the AXE II residues that correspond to the $\lambda 3$ loop. Based on these data, we have formulated the hypothesis that the $\lambda 3$ loop is responsible for restricting the length of the fatty acid that can bind to AXE II. In this work, we have prepared a deletion mutant where part of this loop has been eliminated. This mutant is catalytically active and can hydrolyze long chain fatty acid esters with much greater efficiency than the wild type AXE II.

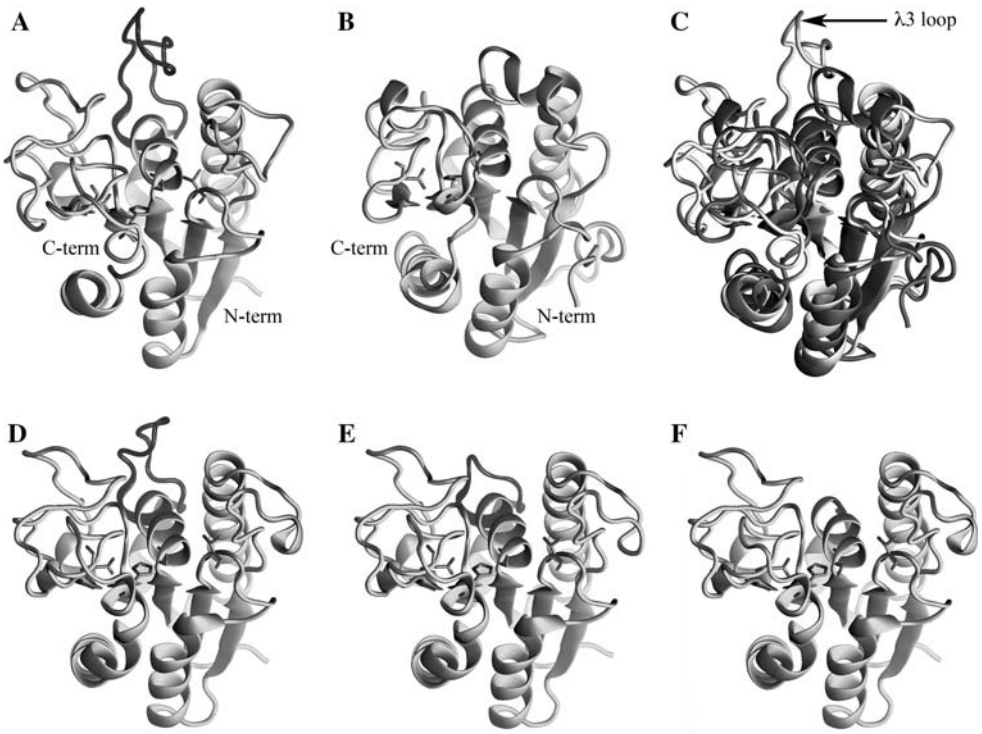

Fig. 1 Tertiary structure representation of AXE II (panel **a**), cutinase (panel **b**) and AXE II mutants (panels **d**, **e** and **f**). Panel **c**: structural superposition of the Cα of AXE II (light gray) and cutinase (dark gray). The catalytic triad residues are displayed by sticks

Fig. 2 Multiple sequence alignment of AXE II from *P. purpurogenum*, cutinase from *F. solani* and AXE II mutants. Shadowed segments correspond to equivalent secondary structures between AXE II and cutinase. Symbols appearing over shadowed areas denote secondary structure type. Secondary structures have been numbered in accordance with Ghosh et al. [8, 9]

Materials and methods

Bioinformatic analysis

Despite of the low sequence identity (less than 20%) showed by AXE II (PDB 1G66) and cutinase (PDB 1CEX), they share a common fold (see Fig. 1c). As a consequence, we decided to use STAMP v4.2 [12] to produce a structural alignment based on a Cα superposition of equivalent residues of both crystal structures. The structural alignment (Fig. 1c) was used to produce a subsequent multiple alignment (see Fig. 2) using three different deletion mutants of AXE II. AXE II mutant models were developed by a comparative modeling procedure using MODELLER v8.2 [13]. The input alignment for MODELLER was computed with ClustalX v1.83 using a PAM45 scoring matrix [14]. As can be seen in Fig. 1, three mutant models (AXEL, AXEV and AXEM) where built using the AXE II crystal structure as template by gap-replacement of the corresponding λ3 loop residues in the input alignment. The deletion lengths where chosen in a way that all deletions do not alter the two alpha helix secondary structure that surround the λ3 loop; the AXEL mutant lacks the whole λ3 loop (Fig. 1d), the AXEM mutant lack residues 104–114 (Fig. 1e) and the AXEV mutant lacks residues 105–110 (Fig. 1f). Ten models were produced for each mutant with five loop refinements per mutant, to obtain a total of 50 models. All resulting models were evaluated with PROSA II z-scores and with the combined potential energy of every conformation [15]. The top scoring models were selected and the integrity of the anchor residues (flanking the deletion) was assessed with PROSAII and Verify3D [16] profiles. To evaluate the structural stability of the selected models and the integrity of their catalytic site, molecular dynamics (MD) simulation protocols were conducted with program NAMD 2.5 [17] using the CHARMM27 force field [18]. After correcting pH and ionic strength to physiological conditions [7, 10] each model, the AXE II and cutinase crystal structures were immersed in a MD system through a water solvation box in periodic boundary conditions. Particle Mesh Ewald (PME) [19] was used to account for long range electrostatic interactions in the NPT thermodynamic ensemble by coupling the system to a Langevin thermal bath [20] and to a barostat. The equilibration of the systems consisted of two stages. During the first stage a 500 ps MD run was performed keeping the protein atoms fixed, while solvent atoms and ions were set free. In the second stage, lateral chains of the amino acids were released maintaining a harmonic constraint (K) of 12.5 Kcal mol^{-1} over the catalytic site Cα atoms. This constraint was scaled by factors of K/2.5 after 2 ns and K/5 after 3 ns, for a total constrained simulation time of 3 ns. Subsequently, all constrains were removed, reaching the stationary state after 300 ps of additional simulation. After this point, a full atom MD simulation of 4 ns was performed collecting frames each 1 ps. The Cα root mean square deviation (RMSD) and the distance between Ser Oγ and His Nε of the catalytic site were calculated for all structures along the MD simulation. The average structures used to proceed with the binding site analysis (BSA) (see below) were calculated by averaging the coordinates of all atoms along the 4 ns trajectory. The resulting average structures were energy minimized by means of a conjugate-gradient algorithm until the force gradient decayed by 100 KJ mol^{-1} nm^{-1}. In order to study whether or not all the λ3 loop deletions could affect the disposition and volume of the AXE II active site, a comparative BSA was performed using the BSA module available in InsightII [21], using default parameters. Briefly, the protein is mapped onto a grid which covers the complete protein space. The grid points are then defined as free points and protein points. The protein points are grid points, within 2 Å from a hydrogen atom or 2.5 Å from a heavy atom. Then, a cubic eraser moves from the outside of the protein toward the center to remove the free points until the opening is too small for it to move forward. Those free points not reached by the eraser are defined as site points. Obtained site points were then rendered as solid surfaces.

Microbial strains

E. coli DH5α was used for cloning. The native and mutant enzymes were expressed in both *Aspergillus nidulans* A722 which lacks the pyrimidine biosynthesis enzyme orotidine monophosphate decarboxylase (kindly supplied by Dr. Rafael Vicuña, Laboratorio de Bioquímica, P. Universidad Católica de Chile) and *Pichia pastoris* GS 115 that lacks the enzyme histidinol dehydrogenase his4 (obtained from the EasySelect™ *Pichia* Expression kit, Invitrogen).

Culture media

The bacteria were grown in LB medium (1% tryptone, 0.5% yeast extract, 0.5% NaCl). For solid media, 1.5% agar was added. Bacterial transformants were selected in Luria medium containing 100 μg/mL Ampicillin.

Aspergillus was grown in a rich medium containing 0.5% yeast extract, and 2% glucose (YEG) or 5% maltose (YEM), and supplemented with 2% agar for solid medium. A minimal medium was also used: per liter, 10% Casaminoacids (DIFCO) (1 g nitrogen), 0.52 g KCl, 0.52 g $MgSO_4 \times 7H_2O$, 1.52 g KH_2PO_4, 5% autoclaved maltose, 400 μL 0.1% *p*-amino benzoic acid, 100 μL Pluronic F 68 and 2 mL Hunter trace salts solution, pH 6.5. Hunter's solution contains (in 100 mL) adjusted to pH 6.5–6.8, 2.2 g $ZnSO_4 \times 7H_2O$, 1.1 g H_3BO_3, 0.5 g $MnCl_2 \times 4H_2O$, 0.5 g $FeSO_4 \times 7H_2O$, 0.16 g $CoCl_2 \times 6H_2O$, 0.16 g $CuSO_4 \times 5H_2O$, 0.11 g $(NH_4)_6Mo_7O_{24} \times 4H_2O$ and 5 g EDTA.

Pichia pastoris GS 115 was grown in the media indicated by the manufacturer of the kit. Clones were grown in YEPD medium (1% yeast extract, 2% peptone and 2% glucose). Selection of transformed yeasts was performed using the antibiotic Zeocin (100 μg/mL) in BMGH minimal medium (1.3% yeast nitrogen base free of amino acids (DIFCO), 4×10^{-5}% biotin, 100 mM potassium phosphate pH 6.0 and 4% glycerol in 1 L). For induction the clones were incubated in BMMH medium (it contains 0.5% methanol instead of glycerol).

Vectors used for transformation

The mutant (plasmid pBA3) was constructed by PCR (see Results) using plasmid pSQ1 as template. The latter was generated as follows: the cDNA sequences of AXE II, the α-amylase promoter from *Aspergillus oryzae* and the glucoamylase terminator from *Aspergillus awamori* were obtained by PCR and used as template with primers JE 86 and JE 87 (see Table 1), obtaining a fusion product of the expected size (~1,600 bp) which was inserted in pBLUEScript and cloned in *E. coli*.

Plasmid ppyrG, containing the orotidine monophosphate decarboxylase gene was used to co-transform *A. nidulans* [22]. pPICZA (3,330 bp) was obtained from Invitrogen and was used to transform *P. pastoris*. This plasmid includes the promoter region of the alcohol oxidase gene (thus allowing for methanol induction), the terminator region of the same gene and the gene for resistance to the antibiotic Zeocin. The cDNA of AXE II was inserted in this plasmid generating pZ3.

Recombinant DNA methodology

Routine plasmid preparations were performed with the "Concert Rapid Purification System" (Gibco-BRL).

Table 1 Primers used in this work

Primer	Sequence	Location[a]	Sense
JE 65	AGACTCGAATTCATGCATTCCAA[b] GTTTTTCGCA	1–2	Forward
JE 66	AGACTCGGTACCCTATTAACCCA[b] GCTTGCTCTTG	705–687	Reverse
JE 86	ACCCCACAGAAGGCATTTATGCA[b] TTCCAAGTTTTT	1–17	Foward
JE 87	GCGAAATGGATTGATTGTCTATT[b] AACCCAGCTTGCTCT	705–678	Reverse
JE 123	CTGTCTGGTCTTCTACAC	3′ end of glucoamylase terminator region	Reverse
JE 124	CCCGAATCGATAGAACTA	5′ end of a-amylase promoter region	Forward
JE 203	GTACAGCTGTCCTCATCG	426–441	Forward
JE 204	GGACAGCTGTACACCACCGCACA GGGC	345–356/295–309	Reverse
JE 205	ACCACCGCACAGGGCCAC	294–309	Reverse
470	ACAATCAATCCATTTCGC	5′ end of the terminator region of glucoamylase	Forward
876	AAATGCCTTCTGTGGGGT	3′end of the promoter region of α-amylase	Reverse

[a] The location refers to the sequence of AXE II cDNA, with exception of JE 123, JE 124, primer 470 and primer 876 used in the heterologous expression in *Aspergillus*

[b] Underlined sequences were introduced for the purpose of this work

Plasmids for sequencing were prepared by means of the Qiagen Plasmid Mini Kit (Quiagen). For extracting DNA from agarose gels, the "Concert Gel Extraction System" (Gibco-BRL) or the "Wizard PCR Preps DNA Purification System" (Promega) were used. All other basic procedures were performed as described by Sambrook and Russell [23].

PCR methods

PCR assay conditions were as follows: 20 mM Tris–HCl pH 8.4, 50 mM KCl, 0.05 mM each of dATP, dGTP, dCTP and dTTP, 2.5 mM $MgCl_2$, 0.06 U of Elongase (Gibco-BRL) and 15 pmoles/μL of the corresponding primers. The amount of template varied according to the experiment. The PCR protocol used consisted of 30 cycles of 1 min denaturation at 94 °C, 1 min hybridization at different temperatures and 1–3 min elongation at 72 °C (depending on the size of the expected fragment), with a final extension step of 10 min at 72 °C.

Heterologous expression

In *A. nidulans*: 100 mL of YEGU medium (0.5% yeast extract, 2% glucose, 0.2% uridine) were inoculated with 2×10^8 spores of *A. nidulans A722* and incubated for 14 h at 30 °C and 300 rpm in a rotary shaker. The mycelium was centrifuged, washed twice with 0.6 M KCl, centrifuged and resuspended in 50 mL of a solution containing 0.12 g Novozyme, 0.25 g $MgSO_4$ and 0.05 g BSA in 0.6 M KCl. The suspension was incubated at 30 °C for 3 h with 50 rpm agitation and filtered through Miracloth.

The filtrate, containing the generated spheroplasts, was centrifuged. The pellet was washed with 40 mL 0.6 M KCl and resuspended in 500 μL 1 M sorbitol adding 125 μL polyethylene glycol (PEG). Three μL of ppyrG and 6 μL of pBA3 (both 1 μg/μL) were mixed with 150 μL of the spheroplast-containing suspension and the mixture was kept in ice for 30 min. Six hundred μL PEG were added dropwise, mixed gently and incubated at room temperature for 15 min. Eight hundred μL 0.6 M KCl were added and the mixture was centrifuged. The supernatant (leaving 300 μL behind) was discarded and the cells were resuspended in this remaining volume. Hundred and 200 μL samples were plated in YEG-KCl (YEG + 0.6 M KCl) and incubated at 37 °C for at least 60 h until the appearance of colonies. Colonies were selected from YEG-KCl plates and grown in YEG medium at 37 °C and 150 rpm for 20 h. The cells were centrifuged and frozen in liquid nitrogen and 450 μL of lysis solution were added (50 mM Tris–HCl pH 7.5, 50 mM EDTA, 3% SDS, 1% 2-mercaptoethanol). The suspension was incubated for 1 h at 65 °C with occasional mixing, and 320 μL cold phenol/chloroform (25:24:1 phenol:chloroform:isoamilic alcohol pH 8.0) were added. After gentle mixing, the suspension was centrifuged. 300 μL of the aqueous phase containing the DNA were separated and added 12 μL 3 M sodium acetate pH 5.2 and 160 μL cold isopropanol. After centrifuging, the pellet was put for 20 min at −20 °C, washed with 200 μL 70% ethanol and dried. The pellet was resuspended in 60 μL DNase free H_2O and used as template for PCR in order to verify the presence of the insert. In addition, for AXE activity estimation, the prospective clones grown in YEM plates for 144 h, were overlayed with methyl umbelliferyl acetate (MUA)-containing agar, and the appearance of fluorescence was observed under UV light after 60 min incubation at room temperature.

In *P. pastoris*: *E. coli* transformed with pZ3 or pPICZA were grown in LB plates containing 0.25% Zeocin for 16 h at 37 °C. Colonies were picked and grown in 2 mL of liquid LB medium with 0.5 mL Zeocin (in duplicates) for 16 h at 37 °C. Fifty μL were used for plasmid extraction and the DNA was linearized with *Dra* I incubating for 1 h at 37 °C. In parallel, 20 μL of *P. pastoris* GS 115 were grown in YEPD for 16 h at 28 °C and stirred at 150 rpm. Two mL of YEPD were inoculated with 20 μL of the previous culture and grown under the same conditions. The cells were centrifuged, the pellet was washed twice with 1 mL of cold sterile water and resuspended in 80 μL 1 M sorbitol. The cells were then mixed with the linearized DNA, and after incubating for 5 min in ice they were subjected to electroporation with a pulse of 1,500 V, 25 μF and 200 Ω. One mL of 1 M sorbitol was added immediately and the cells placed in ice; this was followed by a 2 h incubation at 30 °C. The cells were centrifuged, resuspended in 100 μL 1 M sorbitol, plated in YPDS containing Zeocin (100 μg/mL) and incubated for 3 days at 30 °C for colony formation. AXE activity was determined in the colonies using the same procedure described for *Aspergillus.* The clones selected were resuspended in 1 mL YEPD and were grown for 24 h at 28 °C with agitation. Ten μL of each culture were added to 1 mL of BMGY medium and grown for 18 h. Cells were induced by mixing 10 μL of each culture with 1 mL of BMGY or BMGH media and adding 100 μL of 10% methanol. Methanol addition was continued for several days adding 10 μL pure methanol to each culture every 24 h.

Enzyme activity and protein determinations

Activity was measured using either *p*-nitrophenyl acetate or α-naphtyl derivatives (acetate, caprate and myristate) as substrate as described previously [6, 10]. MUA and

methylumbelliferyl butyrate were utilized for qualitative determinations in 96-well plates. Protein was determined by the method of Bradford [24]. SDS-gel electrophoresis was performed as described by Laemmli [25] and the gels were stained with Coomassie Brilliant Blue R-250 or with silver nitrate [26].

Immunodetection

This method was used for the detection of the heterologous expression products from both *Aspergillus* and *Pichia* transformants using polyclonal antibodies against AXE II produced in rabbits as described previously [10].

Isoelectric point determination

The samples were desalted by ultrafiltration in 10 mM citrate pH 4.0 and subjected to electrophoresis in a Bio-Rad 111 Mini IEF Cell according to the manufacturer's instructions, using ampholytes in the pH range 3–10. The gel was run for 15 min at 100 V, 15 min at 200 V and 60 min at 450 V. The presence of AXE was detected using an overlay of MUA (3 mg were dissolved in 10 mM citrate pH 4 and 1% low melting agarose) and observed under UV light.

Purification of recombinant AXE expressed in *A. nidulans*

Three liter of YEM medium were inoculated with 4×10^8 spores/L (obtained from YEG plates) and grown in an orbital shaker for 69 h at 28 °C and 150 rpm. The culture was filtered and the clear supernatant was concentrated in a Minitan ultrafiltration unit (Millipore). The enzyme was subjected to fractionation in a CMC-50 Sephadex column (25.5 × 1.9 cm) equilibrated with 10 mM citrate pH 4.0. After washing the column with the buffer, the enzyme was eluted with five column volumes of a linear gradient of NaCl (0–150 mM) in the same buffer. A final purification step was performed using a 61 × 1.7 cm column of Sephadex G-50 equilibrated with 50 mM phosphate buffer pH 6.0.

Purification of the recombinant AXE expressed in *P. pastoris*

One liter culture of *P. pastoris* clone GSAm1 was grown in minimal medium for 65 h as described above. The culture supernatant obtained after centrifugation was concentrated by ultrafiltration using a 3 KDa cutoff membrane. The sample was then chromatographed in a 10 mL phenyl agarose column equilibrated in 50 mM citrate buffer pH 4 and 1.2 M ammonium sulfate. After washing with two column volumes of this buffer, elution was performed with a 10 column volume decreasing linear gradient of ammonium sulfate in the same buffer from 1.2 M to 0 M.

Regioselectivity assay

The regioselectivity of AXE II and the mutant were assayed following the method of Biely et al. [27], utilizing monoacetylated 4-nitrophenyl-xylopyranosides as substrates, kindly supplied by Dr. Peter Biely (Bratislava, Slovakia). The enzymes expressed in *Pichia pastoris* were utilized for this experiment.

Results

Structural and multiple sequence alignment

As can be seen in Fig. 2, three major gaps differentiate the AXE II and cutinase sequences. The first major gap, present in AXE II, is located at the N-terminal of both proteins and ranges from R1 to A12 (cutinase). As indicated in Fig. 2b, the secondary structure exhibited by the equivalent segment in cutinase is a loop. The other two gaps are found in cutinase. The second major gap goes from E139 to D154 (cutinase), and collocates with the main secondary structure element that differentiates AXE II from cutinase, the $\lambda 3$ loop (Fig. 2). The third major gap ranges from L175 to Q193, collocating with strand $\beta 8$ of AXE II (Fig. 2). All the AXE II mutants differ from the wild type sequence only in those residues located in the $\lambda 3$ loop that were gap-replaced to produce the desired mutants (Fig. 2).

Comparative modeling of AXE II mutants

Selected AXE II mutant models were obtained (Fig. 1d, e and f) from the comparative modeling step by evaluation of the PROSAII combined z-scores and potential energy of every conformation (see Supplementary Material Fig. 1). The ProsaII and Verify3D profiles (see Supplementary Material Fig. 2) near the deletion zones show no big differences between the models and the AXEII crystal structure. As can be seen in Fig. 1c, a Cα superposition of both AXE II and cutinase crystal structures shows that the main differences between both proteins are mainly constrained to loops, with emphasis in the $\lambda 3$ loop. Figures 1d,

e and f show a tertiary structure render over Cα of the AXEV, AXEM and AXEL mutant models, respectively. Note the extended secondary structure conservation present in all mutant models of AXE II. In order to test the dynamic stability of the AXE II mutant models, a set of MD experiments were performed. As can be seen in Fig. 3a and b, the Cα RMSD calculated along the entire MD never reached 2.5 Å, exhibiting an extensive secondary structure conservation during the simulation (also see Supplementary Material Fig. 3). The distance between the catalytic site Ser Oγ and His Nε obtained was similar to that of AXEII and cutinase (see Fig. 3c and d). The catalytic site distance in the AXEM model showed the most stable behavior fluctuating around 4.5 Å (see Fig. 3d).

Binding site volume analyses (BSA) performed in cutinase, AXE II, and its deletion mutant models are presented in Fig. 4 and Table 2. As seen, the cutinase crystal structure showed an active site volume bigger than that of AXEII crystal structure. The active site volume of all three models showed and increment, the largest being that of the AXEV model, when compared to AXEII. In addition, the resulting AXEV and AXEM active site volumes were similar to the active site volume of cutinase. Note that the AXEM model presented the lowest RMSD value when compared to the cutinase crystal structure (see Supplementary Material Table 1). Since the AXEM model presented both the best integrity of the catalytic site along the MD simulation and a similar active site volume when compared to the cutinase structure, we selected this mutant for further experimental studies.

Preparation of the mutants

The mutant was prepared according to the following strategy. A first PCR reaction was performed using primers JE 123 and JE 124 (see Table 1) and pSQ1 as template. A product of the expected size (1,600 bp) was obtained. A second PCR was performed using the 1,600 bp fragment as template and primers JE 124 and JE 205, obtaining an expected product of 1,090 bp. This fragment was used for a third PCR (JE 124 and JE 204 as primers) and the expected product was obtained. A fourth PCR (primers JE 123 and JE 203) with the 1,600 bp fragment as template gave a 483 bp product (expected). In the fifth PCR, the products of the third and fourth reaction (overlap extension) were used as template (JE 123 and JE 124 as primers) and the expected final product of 1,567 bp was obtained. This product was cloned in pGEM-T and the resulting plasmid (named pBA3) was used to transform *E. coli* DH5α. Four

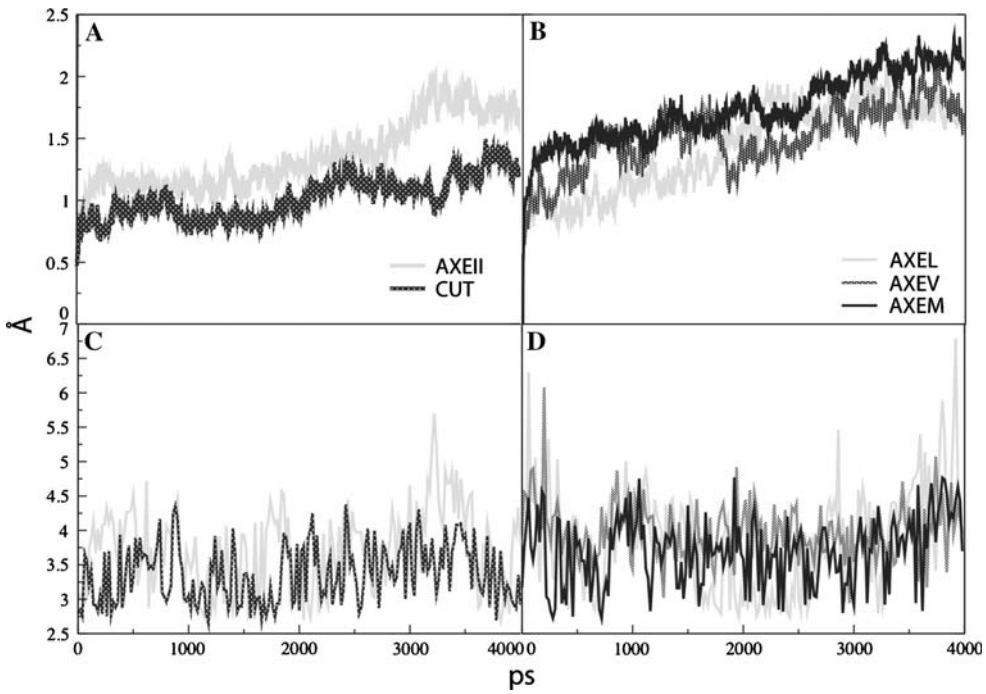

Fig. 3 Trajectory analyses of MD simulations of AXE II, cutinase and AXE II mutants. Panel **a**, plot of Cα RMSD versus the first frame. Grey solid line, AXE II crystal structure; black dotted line, cutinase crystal structure. Panel **b**, plot of Cα RMSD versus the first frame. Grey solid line, AXEL mutant model; black dotted line, AXEV mutant model; black solid line, AXEM mutant model. Panel **c**, distance between Ser Oγ and His Nε of the catalytic site along de MD simulation. Grey solid line, AXE II simulated structure; black dotted line, cutinase simulated structure. Panel **d**, distance between Ser Oγ and His Nε of the catalytic site along de MD simulation. Grey solid line, AXEL mutant model; black dotted line, AXEV mutant model; black solid line, AXEM mutant model

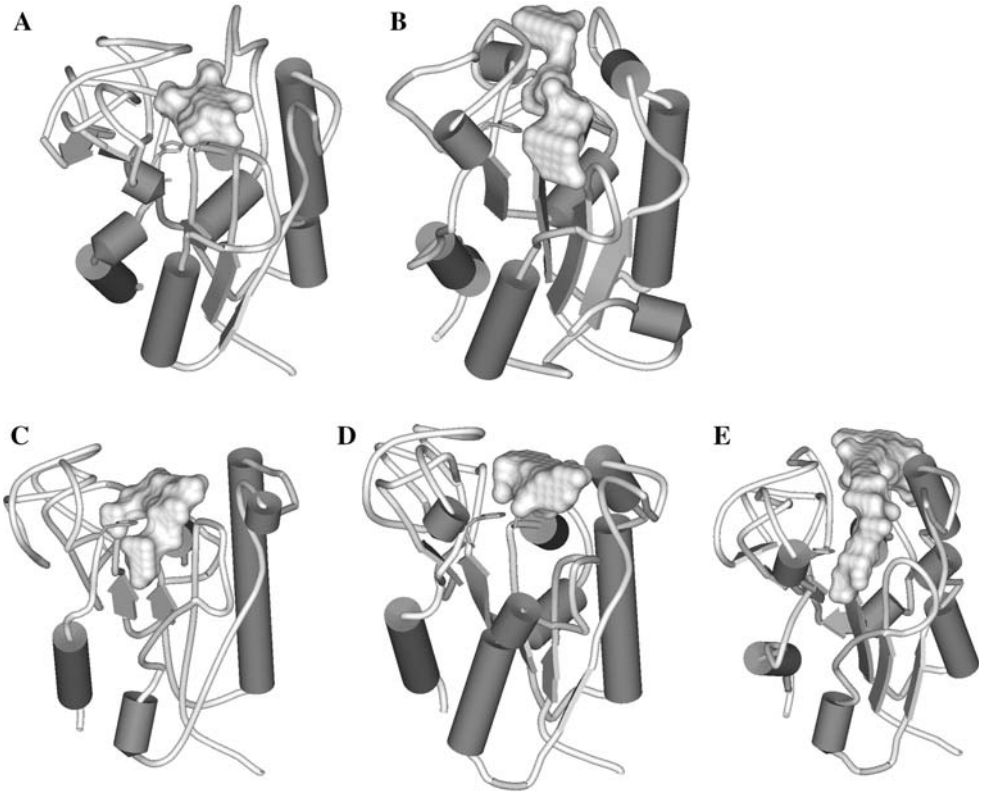

Fig. 4 Representation of AXE II, cutinase and AXE II mutants average minimized structures after a 4 ns MD run, showing a volumetric surface calculated by means of BSA on the binding site of every structure. Residues corresponding to the catalytic triad are indicated by their side chains. Panel **a**; AXE II. Panel **b** cutinase Panels, **c**, **d** and **e**; models of mutants AXEL, AXEM and AXEV, respectively

Table 2 Results of the BSA analyses performed on AXE II, Cutinase and AXE II mutant models from the average minimized structures after a 4 ns MD simulation

Binding site volume (Å^3)	
Structure	Volume
AXEII	73
CUT	111
AXEV	256
AXEM	93
AXEL	109

colonies were analyzed by PCR with primers JE 33 and JE 40 in order to confirm the presence of the insert. The purified plasmid from one of the clones was cut with *Sac I* (only one cut is predicted) and a linear DNA of 4,560 bp (as expected) was obtained in a gel. The insert was sequenced; a base change from G to A was detected at position 609, but this mutation is silent since it also codes for Pro 176.

The heterologous expression of the mutant in *Aspergillus nidulans* A722 was performed as follows. The fungus was co-transformed with plasmids pBA3 and ppyrG. 370 clones were obtained when the transformants were grown in a uridine-free medium. Genomic DNA was extracted from 10 clones and the presence of the insert was verified by PCR. A second PCR reaction was performed using DNA from the positive clones as template and primers JE 124 and JE 205. Four positive clones were selected and grown in a YEM plate. Enzyme activity was detected as fluorescent halos using MUA as substrate. The clone with highest activity (BA3-4) was selected. Transformants containing the gene of the native AXE II were prepared in a similar fashion.

Pichia transformants were obtained as follows. The cDNA of AXE II $\Delta^{104–114}$ was amplified by PCR from pBA3 with primers JE 65 and JE 66 to introduce restriction sites for Kpn1 and EcoR1, respectively. Both the product and pPICZA were treated with these restriction enzymes and ligated. The resulting plasmid (pZ3) was used to transform *E. coli* and the positive clones were selected with Zeocin. Four positive clones were analyzed for the presence of the insert by extracting the plasmids and subjecting them to digestion by EcoR1 and Kpn1. One of them (pPAm1) was used to transform *Pichia pastoris* as described in Methods. Supernatants of cultures of six clones were analyzed for enzyme activity as described above. One of them (clone GSAm1) which showed the highest activity was selected for further work. Transformants of the native AXE II were prepared in a similar fashion.

Characterization of the mutant enzyme

Figure 5 shows an SDS-PAGE of the native and mutant enzymes expressed in *Aspergillus*. The mutant enzyme, as

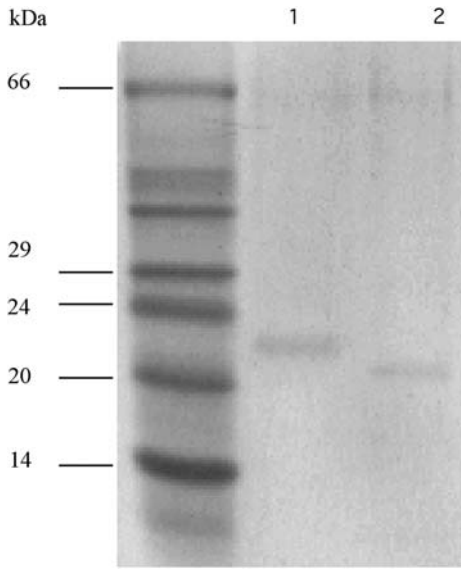

Fig. 5 SDS-PAGE of the purified native (lane 2) and mutant AXE II (lane 3) expressed in *Aspergillus nidulans*. Lane 1: molecular weight standards

expected, is smaller and has a MW of about 21,900. The pI, measured by isoelectrofocusing and zymogram, is ~5.9 (as compared to ~6.8 for recombinant native enzyme) (data not shown). This last enzyme gave a similar pI value to that obtained with the purified enzyme from *P. purpurogenum* (data not shown). The mutant enzyme cross-reacts with AXE II antiserum. Substrate specificity was assayed using three alpha naphtyl esters of different acid lengths. The results are shown in Table 3. While the native recombinant enzyme behaves as established previously for native AXE II [10] with preference for short chain fatty acid esters, the mutant enzyme shows significantly higher activity up to at least a 14 carbon fatty acid ester. The mutant enzyme shows an optimal temperature of 60 °C but it is less stable than the native recombinant protein at 70 °C. Results of substrate specificity obtained with the enzyme expressed in *Pichia pastoris* are similar: the mutant enzyme shows significantly higher activity than the wild type when the substrate used is an ester of 10 or 14 carbon fatty acids. The regioselectivity of the native and mutant enzyme (see Table 4) is similar: both are more active when the acetyl substituent is linked to carbon 2 of the xylose.

Table 3 Substrate specificity of the native recombinant and mutant AXE II

Substrate	Native enzyme U/mg protein[a]		Mutant enzyme U/mg protein[a]	
α-Naphtyl acetate	27.4	26.1	26.8	23.9
α-Naphtyl caprate	1.42	1.5	11.3	12.1
α-Naphtyl myristate	0.67	0.8	12.0	14.3

[a] First column, data from *Aspergillus* transformants; second column, data from *Pichia* transformants

Table 4 Regioselectivity of the native recombinant AXE II and the deletion mutant

Enzyme	Ac-C2[a]	Ac-C3[a]	Ac-C4[a]
Native	1[b]	0.003	0.002
Mutant	1[b]	0.016	0.004

[a] Ac-C2, Ac-C3 and Ac-C4 indicate the number of the xylose carbon to which the acetate group is bound

[b] The results are expressed in relation to the activity towards Ac-C2 which is assigned the value of 1

Discussion

The presence of the λ3 loop in AXE II and its absence in cutinase prompted the formulation of the hypothesis that this loop limits the activity of AXE II to esters of short chain fatty acids. When a structural comparison of AXE II with cutinase is performed (Fig. 1c), the complete α-β sandwich central core of both proteins can be superimposed by Cα trace with an RMSD of 4.6 Å. By adding the loops to this analysis, this value increases to 9.1 Å, indicating that the loops represent the main structural difference between both enzymes. If AXE II and cutinase are aligned (Fig. 2), a high correspondence between the secondary structure elements of AXE II and cutinase are observed, being the loops the most variable segments. The most relevant difference is due to AXE II λ3 loop, not present in cutinase, which has been described as a boundary of the AXE II binding site [9]. In order to evaluate the effect of the AXE II λ3 loop deletions, a set of comparative models was produced by gap replacing of AXE II sequence. Thus, three different mutant models were developed as can be seen in Fig. 1. Despite of the high secondary structure conservation present in all models, a series of MD experiments were carried out to confirm their structural stability. For this purpose, a 4 ns all-atom MD simulation was performed. To test for any structural change at the active site that could be related to the deletion of λ3 loop residues, a set of BSA analyses was performed on cutinase, AXE II and the mutant models. As seen in Fig. 4 and supplementary material Table 1 , all mutant models predict changes in the active site volume, the AXEM model being the one that was closest to the structure of cutinase. All together, our results suggested that the AXEM model is the AXE II mutant that satisfies our hypothetical premise, accomplishing the structural and biophysical constrains that help retain the catalytic activity of this enzyme.

The experimental results support the hypothesis that the $\lambda 3$ loop limits the substrate specificity of AXE II and confirm the predictions of the model. The availability of an esterase of broad substrate specificity may be of potential interest for biotechnological applications such as the synthesis of long chain fatty acid esters of secondary alcohols.

Acknowledgements This work was supported by grants from FONDECYT (N°1040201, 1070368 and 980004) and Universidad Andrés Bello (N° 19-03 and 03-05/R). The CBUC wants to acknowledge the support of the Fundación Chilena para Biología Celular and the Fundación Ciencia para la Vida.

References

1. Joseleau JP, Comtat J, Ruel K (1992) Prog Biotechnol 7:1
2. Biely P (1985) Trends Biotechnol 3:286
3. Sunna A, Antranikian G (1997) Crit Rev Biotechnol 17:39
4. Williamson G, Kroon PA, Faulds CB (1998) Microbiology 144(Pt 8):2011
5. Chavez R, Bull P, Eyzaguirre J (2006) J Biotechnol 123:413
6. Gordillo F, Caputo V, Peirano A, Chavez R, Van Beeumen J, Vandenberghe I, Claeyssens M, Bull P, Ravanal MC, Eyzaguirre J (2006) Mycol Res 110:1129
7. Gutierrez R, Cederlund E, Hjelmqvist L, Peirano A, Herrera F, Ghosh D, Duax W, Jornvall H, Eyzaguirre J (1998) FEBS Lett 423:35
8. Ghosh D, Erman M, Sawicki M, Lala P, Weeks DR, Li N, Pangborn W, Thiel DJ, Jornvall H, Gutierrez R, Eyzaguirre J (1999) Acta Crystallogr D Biol Crystallogr 55:779
9. Ghosh D, Sawicki M, Lala P, Erman M, Pangborn W, Eyzaguirre J, Gutierrez R, Jornvall H, Thiel DJ (2001) J Biol Chem 276:11159
10. Egaña L, Gutierrez R, Caputo V, Peirano A, Steiner J, Eyzaguirre J (1996) Biotechnol Appl Biochem 24(Pt 1):33
11. Carvalho CM, Aires-Barros MR, Cabral JM (1999) Biotechnol Bioeng 66:17
12. Russell RB, Barton GJ (1992) Proteins 14:309
13. Sali A, Blundell TL (1993) J Mol Biol 234:779
14. Aiyar A (2000) Methods Mol Biol 132:221
15. Sippl MJ (1993) Proteins 17:355
16. Eisenberg D, Luthy R, Bowie JU (1997) Meth Enzymol 277:396
17. Phillips JC, Braun R, Wang W, Gumbart J, Tajkhorshid E, Villa E, Chipot C, Skeel RD, Kale L, Schulten K (2005) J Comput Chem 26:1781
18. MacKerell AD Jr, Banavali N, Foloppe N (2000) Biopolymers 56:257
19. Darden T, Perera L, Li L, Pedersen L (1999) Structure 7:R55
20. Adelman SA, Doll JD (1976) J Chem Phys 64:2375
21. InsightII v 2001, Accelrys Inc., San Diego, USA, (2000–2006)
22. Oakley BR, Rinehart JE, Mitchell BL, Oakley CE, Carmona C, Gray GL, May GS (1987) Gene 61:385
23. Sambrook J, Russell DW (2001) Molecular cloning: a laboratory manual. Cold Spring Harbor Laboratory Press, Cold Spring Harbor, New York
24. Bradford MM (1976) Anal Biochem 72:248
25. Laemmli UK, Beguin F, Gujer-Kellenberger G (1970) J Mol Biol 47:69
26. Bollag DM, Rozycki MD, Edelstein.g SJ (1996) Protein methods. Wiley Publishers, New York
27. Biely P, Mastihubova M, la Grange DC, van Zyl WH, Prior BA (2004) Anal Biochem 332:109